Proceedings of the 2024 Winter Simulation Conference
H. Lam, E. Azar, D. Batur, S. Gao, W. Xie, S. R. Hunter, and M. D. Rossetti, eds.

A NEURAL NETWORK APPLICATION FOR NON-GYROSCOPE BASED AIRCRAFT ATTITUDE DETERMINATION

Raul de Celis[1], and Luis Cadarso[1]

[1]Aerospace Systems and Transport Research Group, Rey Juan Carlos University, Fuenlabrada, Madrid, SPAIN

ABSTRACT

Aircraft accurate navigation and control depends on the estimation framework concerning attitude and position. Aircraft rotation can be obtained, by measuring two different vectors, for instance, gravity and velocity, in two distinct reference coordinated systems: body and inertial local horizon axes. The inertial reference frame's velocity vector is determined using Global Navigation Satellite Systems sensors, while the body reference frame's velocity vector is obtained through integrating accelerometer measurements. To estimate gravity vector in the body-fixed reference frame, an approach is introduced, based on a neural network that determines aircraft aerodynamic forces. Through the derivation of flight dynamics equations, the vector of gravity is finally determined. The combination of these vectors facilitates the body rotation determination. Simulations, employing nonlinear flight dynamics models, demonstrate that accurate aircraft attitude determination is attainable through the integration of just accelerometers, Global Navigation Satellite Systems sensors, and the proposed methodology.

1 INTRODUCTION

Attaining precision in attitude data is crucial for navigation and control, and the literature has explored various sensor inputs for attitude estimation (Crassidis et al. 2007). The effectiveness of navigation systems is intricately linked to the precision of components, including inertial measurement units (Zhu et al. 2019).

Typically, achieving accurate attitude determination involves using costly and bulky units like accelerometers, fiber optic or laser gyros, or their equivalent MEMS devices. Furthermore, these equipment costs can become prohibitive during high-demand maneuvers, as sensor quality requirements are increased.

Determining air vehicles attitude often involves integrating its angular velocities (pitch, roll, and yaw) from an initial condition and propagating them in time. An approach for attitude estimation, outlined by (Eure et al. 2013), involves post processing inflight recorded data in a scaled commercial Unmanned Air Vehicle (UAV) using a cost-effective Inertial Navigation System (INS). Their UAV attitude meassurements rely on magnetometer, MEMS gyro, pitot tube and accelerometer inputs. However, this approach often falls short of meeting precision requirements when using budget-friendly sensors, but recently they appear to increase accuracy. For example, (Yin et al. 2022) developed an affordable attitude control system combining low-cost microcontroller and MEMS sensors. This becomes crucial in UAV applications where cost reduction is essential or vehicle re-utilization is impractical, such as vehicles used for some military applications. Consequently, low-cost attitude determination systems play a pivotal role.

vector of gravity use in attitude determination tasks is common in satellites, (Sun et al. 2022), but not so much in aircraft tasks. A system for attitude determination measuring two nonzero, non-colinear vectors—using gravity and the Earth's magnetic field is proposed in (Gebre-Egziabher et al. 2000) and more recently in (de Celis and Cadarso 2018), where vector of gravity is employed for attitude determination.

According to (Henkel and Iafrancesco 2014), cost-effective GNSS sensors and antennas can provide precise attitude and non-drifted position data, but their precision is not consistent. Inertial sensors, on the other hand, are resilient to GNSS signal interruptions and highly accurate over small durations, enabling a

robust cycle slip correction. However, non-expensive INS are susceptible to significant drift. An integrated attitude and position methodology that incorporates an accelerometer, a gyro and two GNSS devices is proposed. This strategy results in a position accuracy of 1 m and a heading precision of 0.25°/standard length [m]. GNSS constellations have been widely used for attitude determination in aircraft (Raskaliyev et al. 2020). Similar advancements can be found in space vehicles, as demonstrated in (Springmann and Cutler 2014).

An alternative method for non-gyroscopes attitude determination involves utilizing an array of accelerometers to address the six degrees of freedom in the dynamic equations. This approach necessitates a minimum of six accelerometers (at least two of each, separated by a relative distance, on each of the axes of the coordinated system). Processing information from the accelerometer array requires the application of algorithmic regression, as detailed in (Pachter et al. 2013).

Machine Learning (ML) is an emerging field that leverages statistical algorithms to analyze and learn from data, aiming to make predictions or decisions based on that data. In this research context, ML algorithms, and specifically neural networks can be employed in estimating aircraft aerodynamic forces, to employ them together with flight dynamics equations in order to determine vector of gravity, which is crucial for accurate attitude determination. One key advantage of using ML in this context is its ability to obviate the need for an in-depth understanding of the physical-mathematical foundations of aircraft aerodynamics (de Celis and Cadarso 2023). The ML algorithm can be trained or calibrated using input data, such as simulated or experimental data, to learn the relationship between accelerations, velocities and aerodynamic coefficients. Once trained, the algorithm is used in real-time to determine vector of gravity, providing valuable information for a GNC (Guidance, Navigation, and Control) device. With the rise of UAVs, artificial intelligence-based techniques, particularly neural networks, have become essential for automating flight paths (Pang et al. 2019), (Nawaz et al. 2020). Some approaches even incorporate reinforcement learning by analyzing historical flight trajectory data (Azar et al. 2021). ML-based fault-tolerant systems have been developed for aircraft, using neural networks to adapt to actuator failures (Yu et al. 2017). ML applications for spacecraft are also being explored, including optical navigation and other areas (Silvestrini, S and Lavagna, M). This has the potential to significantly enhance the accuracy and reliability of the GNC system, critical for the safe operation of aerospace vehicles. In summary, artificial intelligence and neural networks are finding practical applications in aeronautics, from satellite data analysis to improving the performance and safety of various vehicles and systems. This underscores their potential to enhance aviation and aerospace technologies.

In conclusion, the use of Machine Learning (ML) for resolving aerodynamic forces determination problem offers a promising avenue for improving precision and reliability in attitude determination. Despite skepticism, the examples provided demonstrate the growing body of evidence supporting the value of AI-based algorithms in enhancing aviation and aerospace technologies. ML holds the potential to revolutionize aerospace engineering by providing efficient and effective methods for accurate attitude determination, ensuring the safety and precision of aerospace vehicles.

In the methodology proposed in this study, two magnitudes—gravity and velocity vectors—are meassured and used to obtain attitude for UAVs. These vectors are acquired in two different coordinated systems using a strap-down accelerometer and a GNSS sensor and then processed in a neural network in order to determine the magnitudes for attitude determination.

1.1 Contributions

This paper presents two primary contributions. Firstly, it introduces an algorithm designed to eliminate the need for gyroscopes in attitude calculation. This work establish the first steps for future research, which should include the reduction of the number of sensors used on the aircraft or even hybridize this approach, as a backup or health monitoring, with traditional sensors such as gyroscopes. The central concept is to reduce the cost of attitude sensors and potentially enhance attitude estimation by employing neural network based techniques particularly tailored for cost-effective UAV applications. This is crucial

in scenarios where the expense of accurate sensors for attitude determination, such as gyroscopes or sensor arrays, is prohibitive. The proposed method remains applicable even for compact vehicles, as opposed to a sensor array approaches, where accommodating an array of accelerometers may be challenging due to space constraints.

Secondly, the paper proposes an estimation method specifically developed to determine the vector of gravity in the body frame using machine learning techniques, more concretely neural networks. Nonlinear flight computer simulations are conducted to determine the aircraft's attitude and compare it with the estimated results. The paper emphasizes the significance of the proposed solution for the navigation, guidance, and control of unmanned air vehicles during flight.

The next paper sections are structured as follows. Section 2 provides a detailed description of the problem. Section 3 is dedicated to vector of gravity estimation. The algorithm for attitude determination is outlined in Section 4. Sensor models and Flight dynamics are discussed in Section 5. Simulation results are outlined in Section 6. The paper concludes with a summary and references.

2 PRELIMINARY CONSIDERATIONS

Attitude calculation is a pivotal aspect of aircraft engineering, influencing maneuvers that alter vehicle trajectory through the effects of aerodynamic forces. These forces, in turn, are directly influenced by the Euler angles of the airship. Additionally, determining the attitude of aircraft is essential for assessing the magnitude of aerodynamic forces and executing vital maneuvers like take-off and landing. Consequently, the development of algorithms to enhance attitude calculation forms a fundamental aspect of precise GNC (guidance, navigation and control) research.

An approach used for attitude determination entails calculating it from the direction cosine matrix (DCM), which defines the complete rotation of a body between two reference frames. To derive this DCM, a geometric plane characterized in both reference trihedra needs to be established. Each geometric plane is defined by two vectors. Thus, by having knowledge of these pair of vectors represented in their respective coordinated systems, the DCM can be obtained.

2.1 Aircraft Model

The simulated aircraft is designed to emulate the characteristics of a conventional 'V-tail' UAV. It comprises a fixed wing with a 1.55 meters wingspan and a 1.25 meters length cylindrical body. The fixed wing is equipped with ailerons for control, and the aircraft features a pair of 'ruddervators' with a wingspan of 0.65 meters, each equipped with its corresponding set of control surfaces. There are a total of four independent control surfaces, each capable of individual actuation by adjusting them to specific angles.

This configuration, resembling the classical 'V-tail' UAV, is not uncommon and is employed by certain commercial UAVs currently available on the market. Examples include the CAIG Wing Loong II, the CASC Rainbow CH-4, and the General Atomics MQ-9 Reaper (Zountouridou et al. 2023). The adoption of this configuration in commercial UAVs is primarily driven by considerations of cost-effectiveness in actuation systems, weight advantages, and aerodynamic simplicity.

2.2 Coordinate Systems of Axis

Two distinct coordinate systems are utilized to represent moments and forces: the North-East-Down (NED) axes and the Body (B) axes, as it is shown in Figure 1. The NED axes, have their origin at the takeoff point, $\overrightarrow{x_{NED}}$ pointing to the north, $\overrightarrow{z_{NED}}$ perpendicular to $\overrightarrow{x_{NED}}$ and pointing to nadir, and $\overrightarrow{y_{NED}}$ forming a clockwise coordinated system. In contrast, the Body axes, denoted by the sub-index B, have $\overrightarrow{x_B}$ oriented forward within the UAV's symmetry plane, $\overrightarrow{z_B}$ perpendicular to $\overrightarrow{x_B}$ pointing downward and within the symmetry plane, and $\overrightarrow{y_B}$ forming a clockwise coordinated system. The origin of the Body axes is located at the center of mass of the UAV.

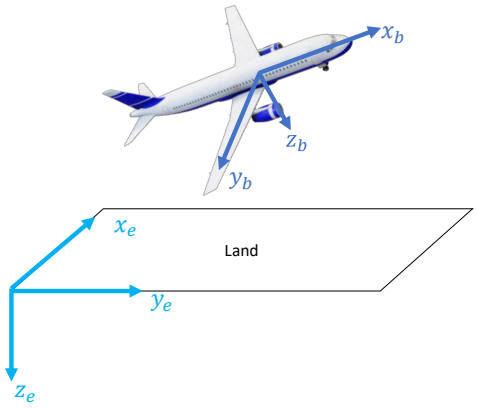

Figure 1: Systems of axes.

2.3 Definition of Trivially Calculated Vectors

The velocity vector can be calculated directly using sensor measurements within the NED trihedron, if the UAV is equipped with a GNSS sensor. The resulting velocity vector in NED is denoted as $\overrightarrow{v_{NED}} = [v_{x_{NED}}, v_{y_{NED}}, v_{z_{NED}}]^T$, specifying the velocity components along the NED axes.

Similarly, an equivalent velocity vector in the body trihedron can be derived from accelerometers installed on the UAV, with one accelerometer along each axis. These accelerometers measure acceleration, and by integrating each component over time, the velocity vector is obtained, as detailed in 1. Here, a_{x_B}, a_{y_B}, and a_{z_B} represent the components of acceleration in the body coordinated system, and $\overrightarrow{\omega_b}$ signifies angular velocity in the body axis.

$$\overrightarrow{v_B} = \overrightarrow{v_B}|_{t=0} + \int \left[[a_{x_B}, a_{y_B}, a_{z_B}]^T + \overrightarrow{\omega_b} \times \overrightarrow{v_B} \right] dt \tag{1}$$

To describe the rotation, an additional vector expressed in two distinct reference frames is essential. The determination in the NED coordinated system of the vector of gravity involves a vector parallel to $\overrightarrow{z_{NED}}$, denoted as $\overrightarrow{g_{NED}} = g[0,0,1]^T$. Here, g signifies the constant acceleration due to gravity, maintained at $9.81 m/s^2$ throughout this paper. It is important to acknowledge that precision can be improved by incorporating more advanced models; for instance the vector of gravity can be modeled based on the UAV's latitude and longitude.

The fundamental aspect of the presented attitude calculation approach relies on knowing the vector of gravity in the body reference frame. Techniques for computing this vector of gravity are outlined in (Mizell 2003). One approach involves acquiring the constant element of the acceleration through the application of a low-pass filter. The jerk in the body reference frame is derived from acceleration, then integrated to derive the variable component of acceleration. However, employing this approach becomes impractical as the aircraft's angular rates increase. Other technique for obtaining the vector of gravity involves integrating the mechanization equations (Savage et al. 2000) and controlling the resulting conditions. Yet, this method also necessitates the use of gyros. In the subsequent section, an alternative estimation technique, applicable to both stationary and rotating aircraft, eliminating the necessity for gyroscopes, will be introduced.

3 ESTIMATION OF VECTOR OF GRAVITY

The vector of gravity estimation strategy introduced in this context is designed to suit the unique characteristics of the aerial platform for which it is intended. This indicates that the strategy needs to be personalized for the specific aircraft under consideration, taking into account factors such as the vehicle's mass distribution and geometry. The modeling process involves acquiring data from flight dynamics conditions. The approach leads to an onboard vector of gravity estimator utilizing accelerometer and GNSS measurements under specified conditions. The estimation methodology depicted in this section and in 5 and 6, is specifically tailored for a fixed-wing aircraft featuring two 'V' tail control surfaces, designated as an Unmanned Air Vehicle. Nevertheless, leveraging the pertinent flight mechanics equations allows for its adaptation for use with other aircraft types. The represented vector of gravity can be expressed as $\overrightarrow{g_B} = [g_{x_B}, g_{y_B}, g_{z_B}]^T$, specifying its components in the body coordinated system.

The fundamental idea behind the provided estimator is that the vector of gravity can be expressed as the disparity between the acceleration ($\overrightarrow{A_B}$) and an approximation of the aerodynamic forces acceleration, expressed in the body axes. This approximation is linked to the precision of the estimations for aerodynamic parameters. Equation 2 delineates the gravity estimator as a specific instance of the Newton-Euler equations, where m denotes the mass of the aircraft and $\overrightarrow{F_{ai}}$ represents passive and active aerodynamic and inertial forces.

$$\overrightarrow{g_B} = \overrightarrow{A_B} - \frac{\overrightarrow{F_{ai}}}{m} \tag{2}$$

To estimate $\overrightarrow{g_B}$ and $\overrightarrow{F_{ai}}$, only data obtained from accelerometers and GNSS sensors can be employed. The angle between the aerodynamic velocity vector and $\overrightarrow{x_B}$, namely total angle of yaw ($\alpha = acos\,[\overrightarrow{v_B} \cdot \overrightarrow{x_B} / |\overrightarrow{v_B}|]$) , and the Mach number ($M = |\overrightarrow{v_B}| / a(z_{NED})$), a dimensionless measure of speed, are calculated from accelerometer data. Those are critical for restitution of attitude calculations. This algorithm is based solely on the vector $\overrightarrow{v_B}$. This assumption holds true for low attack angles, which is the typical scenario in flights as those explained in this paper.

To compute the Mach number, the speed of sound can be estimated as a function of altitude ($a(z_{NED})$) using the International Standard Atmosphere (ISA) model, widely accepted in aviation. Given that altitude remains nearly constant in our simulations, it can be simplified in neural network inputs. Also wind conditions are neglected for this preliminary study, in future works, the information from GNSS sensors could be hybridized with wind models and information from other conventional sensors. Passive aerodynamic and inertial forces ($\overrightarrow{F_{ai}}$) are calculated according to 3:

$$\overrightarrow{F_{ai}} = \overrightarrow{L} + \overrightarrow{D} + \overrightarrow{P} + \overrightarrow{T} + \overrightarrow{C} + \overrightarrow{CF} + \overrightarrow{M_F}, \tag{3}$$

where $\overrightarrow{L}$ signifies the lift force, $\overrightarrow{D}$ denotes the drag force; $\overrightarrow{P}$ represents the pitch damping force; $\overrightarrow{M_F}$ refers to the Magnus force; $\overrightarrow{T}$ stands for the thrust force; $\overrightarrow{CF}$ accounts for the control surfaces forces, and $\overrightarrow{C}$ denotes the Coriolis force.

Each of these forces is estimated by a non-linear flight dynamics model developed in (de Celis et al. 2017). They rely on the external geometry of the aircraft and can be computed through computational fluid dynamics or wind tunnel experiments, or data from real flights. The model is configured to display non-deterministic results in each simulation, so when using the neural network, we will try to mitigate that variability. Note that the development of this model is beyond the scope of this paper; therefore, forces are considered output data for our neural network, functions of vector $\overrightarrow{v_B}$. The preceding mathematical derivation reveals that the vector of gravity in body axes ($\overrightarrow{g_B}$) can be estimated solely by utilizing accelerometer measurements, and a neural network that will feed the values for the forces. The development of this neural network is explained in the following subsection.

3.1 Estimations through Neural Networks

The values of $\overrightarrow{D}$, $\overrightarrow{L}$, $\overrightarrow{M_F}$, $\overrightarrow{P}$, $\overrightarrow{C}$, $\overrightarrow{T}$, and $\overrightarrow{CF}$ at each time during the aircraft's trajectory are computed using Neural Networks (NN). Employing the computed values, utilizing them as inputs and outputs for a self-learning mechanism with the goal of achieving high accuracy in the determination process.

Machine Learning approaches, particularly Neural Networks, have been integrated into both classical and modern Guidance, Navigation, and Control (GNC) applications (see (de Celis and Cadarso 2023)). The primary advantage of Neural Networks lies in their ability for acquiring knowledge of flight dynamics equations, providing a unique advantage compared to alternative approximations. This capability allows for flight prediction without requiring an in-depth understanding of the underlying physics, allowing for the replication of the force determination procedure beyond predetermined operational locations. It's worth noting that Neural Networks demonstrate successful outcomes in solving nonlinear equations, even in the presence of uncertainty (de Celis and Cadarso 2023).

To predict the expected force values, several Neural Networks are employed. Three distinct strategies showcase the suitability of the presented methodology, amalgamating Neural Networks with flight dynamics techniques. Each strategy undergoes a hyperparameter study (de Celis and Cadarso 2023), where the key challenge lies in finding the right balance between training time and result correlation to avoid overfitting. The study determines parameters including the number and configuration of neurons, the volume of training and validation data, the maximum number of epochs, the gradient decay factor, the validation frequency, and the initial learning rate. These parameters are defined as 1000, 0.95, 9.5, and 0.0025, respectively, based on insights from the existing literature. It is important to highlight that augmenting the number of neurons or layers results in a longer computation time with only a slight reduction in approximation error. The three strategies are as follows:

- Strategy 1: A two-layer neural network with 150 sigmoid neurons in the hidden layer and a linear output neuron is defined.
- Strategy 2: Similar to Strategy 1, but with 250 neurons in the hidden layer.
- Method 3: Similar to Strategy 1, but with 400 neurons in the hidden layer.

The input vector for the Neural Network (NN) comprises the three components of the $\overrightarrow{v_b}$ vector, directly derived from accelerometer measurements. The targets consist of the values of $\overrightarrow{D}$, $\overrightarrow{L}$, $\overrightarrow{M_F}$, $\overrightarrow{P}$, $\overrightarrow{C}$, $\overrightarrow{T}$, and $\overrightarrow{CF}$. This dataset is obtained from simulations using the previously introduced non-linear flight dynamics model.

To replicate flight dynamics during training, ideal values for the components of $\overrightarrow{F_{ai}}$ must be determined for each accelerometer measurement. For the proposed problem, one million different simulations have been generated, creating diverse cases for the three inputs and seven outputs of the neural network. Different initial and boundary conditions are used to reduce bias and prevent overfitting.

Three back-propagation methods—Scaled Conjugate Gradient (SCG) (Møller 1993), Bayesian regularization (BR) (MacKay 1992), and Levenberg-Marquardt backpropagation (LM) (Moré 2006)—are employed during the training process. The selection of these methods is based on a literature review (de Celis and Cadarso 2023). The training data accounts for 70% of the total, with 15% set aside for validation purposes.

Nine distinct combinations of training approaches and algorithms are evaluated, considering Mean Squared Error (MSE) and Regression parameter values for performance assessment. MSE represents the average squared discrepancy between outputs and objectives, with lower values indicating reduced errors. The Regression parameter measures the correlation between outputs and objectives, with a value of 1 indicating a tight association.

The training procedures have a maximum of 1000 iterations, and epochs are used to classify the data. Training halts automatically when generalization stops improving or when adaptive weight minimization (regularization) is reached. Mean Average Error (MAE) is employed to manage overfitting.

The trained neural network (NN) is evaluated using independent data, which constitutes 15% of the total dataset. The computational cost associated with the training process remains feasible for standard hardware. The numerical outcomes of the training process, encompassing Regression parameter values and Mean Squared Error (MSE) for strategies 1, 2 and 3, are succinctly presented in Table 1. The "set" column designates whether the data pertains to training (70%), validation (15%), or testing (15%). The training algorithm is explicitly specified in the next column, while the MSE and Regression results for each strategy follow in the subsequent columns.

Table 1: Results of quality parameters for the Neural Network post-training.

		Strategy 1		Strategy 2		Strategy 3	
		MSE	Reg.	MSE	Reg.	MSE	Reg.
SCG	Train	3.23E-03	9.24E-02	2.06E-03	5.52E-01	3.01E-03	3.29E-01
	Validation	2.86E-03	1.07E-01	2.77E-03	5.36E-01	3.03E-03	3.15E-01
	Test	3.33E-03	1.04E-01	1.95E-03	4.96E-01	3.05E-03	3.10E-01
BR	Train	2.48E-04	9.18E-01	2.38E-04	9.82E-01	6.82E-04	9.85E-01
	Validation	2.92E-04	9.85E-01	1.81E-04	9.99E-01	6.61E-04	9.88E-01
	Test	2.52E-04	9.85E-01	1.86E-04	9.98E-01	5.64E-05	9.89E-01
LM	Train	6.50E-04	9.84E-01	5.12E-04	9.84E-01	3.68E-04	9.76E-01
	Validation	6.40E-04	9.88E-01	4.86E-04	9.57E-01	3.15E-04	9.99E-01
	Test	6.80E-04	9.94E-01	5.16E-04	9.78E-01	3.35E-04	9.86E-01

The most favorable overall outcome is achieved with Strategy 2 using the Bayesian regularization (BR) algorithm, yielding a Regression value of 0.998 and MSE value of $1.86 \cdot 10^{-4}$, as detailed in Table 1. Comparable results are observed for the other two strategies under the BR algorithm. However, outcomes for the Scaled Conjugate Gradient (SCG) method are notably unsatisfactory, suggesting its unsuitability for this GNC purpose.

In summary, the LM and BR techniques produce commendable results, particularly with increased network complexity. However, when complexity is reduced, the BR algorithm outperforms LM. Nevertheless, the SCG method demonstrates ineffectiveness for this application, with outcomes lagging by two or three orders of magnitude compared to the others.

4 ATTITUDE RESTITUTION

Attitude restitution can be accomplished by resolving the classical Wahba's problem, as elucidated in (Wahba 1965). The inputs for this problem are outlined as follows. An orthonormal basis is established in NED and B axis systems. This orthonormal basis is defined by expressions 4 and 5 employing unit vectors $\vec{i}, \vec{j}$, and $\vec{k}$ expressed in both bases.

$$\overrightarrow{i_{NED}} = \frac{\overrightarrow{v_{NED}}}{\|\overrightarrow{v_{NED}}\|}, \quad \overrightarrow{j_{NED}} = \frac{\overrightarrow{v_{NED}} \times \overrightarrow{g_{NED}}}{\|\overrightarrow{v_{NED}} \times \overrightarrow{g_{NED}}\|}, \quad \overrightarrow{k_{NED}} = \frac{\overrightarrow{i_{NED}} \times \overrightarrow{j_{NED}}}{\left\|\overrightarrow{i_{NED}} \times \overrightarrow{j_{NED}}\right\|} \tag{4}$$

$$\overrightarrow{i_B} = \frac{\overrightarrow{v_B}}{\|\overrightarrow{v_B}\|}, \quad \overrightarrow{j_B} = \frac{\overrightarrow{v_B} \times \overrightarrow{g_B}}{\|\overrightarrow{v_B} \times \overrightarrow{g_B}\|}, \quad \overrightarrow{k_B} = \frac{\overrightarrow{i_B} \times \overrightarrow{j_B}}{\left\|\overrightarrow{i_B} \times \overrightarrow{j_B}\right\|} \tag{5}$$

Upon establishing an orthonormal basis in the two axis systems, the expression for determining the Direction Cosine Matrix (DCM) is given in 6. Here, $\left[\overrightarrow{i_B}, \overrightarrow{j_B}, \overrightarrow{k_B}\right]$ denotes a $3x3$ square matrix consisting of orthonormal vectors in the body reference frame, $\left[\overrightarrow{i_{NED}}, \overrightarrow{j_{NED}}, \overrightarrow{k_{NED}}\right]$ represents the same concept in the NED reference frame, and $DCM_{B,NED}$ stands for the director cosine matrix that transforms the NED coordinated system into the body coordinated system.

$$DCM_{B,NED} = \left[\overrightarrow{i_B}, \overrightarrow{j_B}, \overrightarrow{k_B}\right]^{-1} \left[\overrightarrow{i_{NED}}, \overrightarrow{j_{NED}}, \overrightarrow{k_{NED}}\right] \tag{6}$$

After acquiring the Direction Cosine Matrix (DCM), it becomes necessary to define the rotation. The most appropriate approach for expressing this rotation is through quaternions $[q_0, q_1, q_2, q_3]$, as they mitigate the risk of encountering singularities on the rotation poles. The matrix equation linking quaternions and $DCM_{B,NED}$ is illustrated in 7.

$$DCM_{B,NED} = \begin{bmatrix} q_0^2+q_1^2-q_2^2-q_3^2 & 2(q_1q_2+q_0q_3) & 2(q_1q_3-q_0q_2) \\ 2(q_1q_2-q_0q_3) & q_0^2-q_1^2+q_2^2-q_3^2 & 2(q_2q_3+q_0q_1) \\ 2(q_1q_3+q_0q_2) & 2(q_2q_3-q_0q_1) & q_0^2-q_1^2-q_2^2+q_3^2 \end{bmatrix} \tag{7}$$

Quaternions are recognized for their ability to express rotations without encountering singularities, although conceptually, they can be challenging to visualize. A different and simpler method to describe these rotations involves Euler angles. In particular, the prevailing rotation used in aerospace applications is defined by yaw (ψ), pitch (θ) and roll (ϕ) angles. The connections between Euler angles and quaternions are outlined in 8.

$$\phi = atan[\tfrac{2(q_2q_3+q_0q_1)}{q_0^2-q_1^2-q_2^2+q_3^2}], \quad \theta = asin[-2(q_1q_3-q_0q_2)], \quad \psi = atan[\tfrac{2(q_1q_2+q_0q_3)}{q_0^2+q_1^2-q_2^2-q_3^2}] \tag{8}$$

5 FLIGHT DYNAMICS AND SENSOR MODEL

The model shown in (de Celis et al. 2017) is utilized, where the equations of motion are integrated to calculate every single flight trajectory. A series of flight simulations, without wind perturbations, is conducted. Three distinct sets of trajectories are examined, as illustrated in Figure 2. Trajectory sets 1 follows a classical waypoint trajectory; trajectory sets 2 follow clockwise ascent square-closed trajectory; and lastly, trajectory sets 3 follow clockwise descent characterized by an elliptical-closed trajectory. Thrust is adjusted to maintain a constant speed throughout the entire trajectory. In each set of trajectories, the inclination angle fluctuates from 0° to 10° in 2.5° increments.

A second-order system model is employed to simulate accelerometers, with a natural frequency of 250 Hz and a damping factor of 0.75.

GNSS sensors are simulated by introducing white noise with a mean of zero and a maximum absolute value of $m_v = 0.01m/s$ for velocity and $m_p = 3m$ for position.

The sensor modeling is based on relatively affordable equipment, leading to significant errors in measurements. These errors will impact the suitability of the attitude calculation method. Nevertheless, as demonstrated in the subsequent section, the results prove to be adequately accurate for low-cost UAV applications.

6 SIMULATION RESULTS

Simulation results are presented utilizing the nonlinear flight dynamics model (de Celis et al. 2017) to validate the effectiveness of the proposed attitude determination algorithm. The trajectories outlined in the preceding section were executed to facilitate a comparison between real and estimated attitudes. The simulations were conducted on MATLAB/Simulink R2021a, employing a desktop computer.

For the assessment of the estimated attitudes against the real counterparts and the vector of gravity, Figure 3 illustrate the expressions $\phi_{\text{real}} - \phi$, $\theta_{\text{real}} - \theta$, and $\psi_{\text{real}} - \psi$ for attitudes. It is crucial to emphasize that the magnitudes obtained from the algorithms outlined in the previous sections are juxtaposed with the corresponding "real" magnitudes obtained from simulation results.

These illustrations present outcomes for an inclination trajectory angle of 5° across three distinct trajectory types, as specified in Figure 2.

To quantitatively evaluate the error throughout the entire simulated trajectories in each instance, the Root Mean Squared Error (RMSE) for each of the three Euler angles ($RMSE_{\phi}^{IP,Traj_i}$), ($RMSE_{\theta}^{IP,Traj_i}$), and ($RMSE_{\psi}^{IP,Traj_i}$) is computed in 9. This error is contingent on $Traj_i$ (trajectory type) and IP (inclination path angle), σ is the path followed during the trajectory.

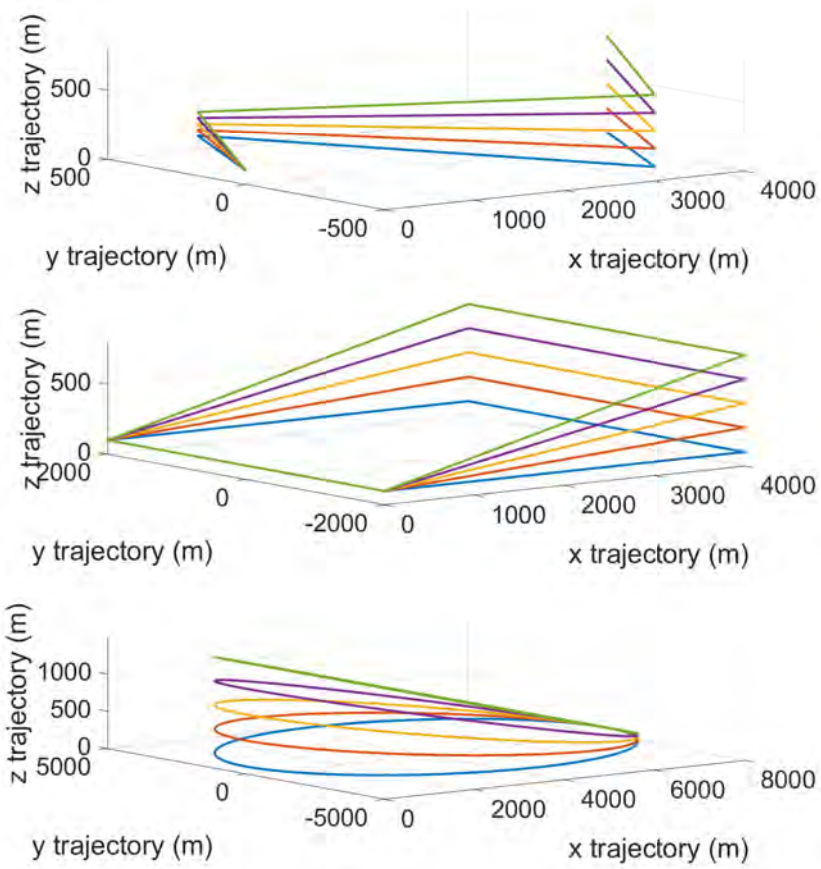

Figure 2: Trajectories 1 (top), 2 (center) and 3 (bottom).

$$RMSE_{\phi}^{IP,Traj_i} = \sqrt{\frac{\oint(\phi_{real}-\phi)^2 d\sigma}{\oint d\sigma}}, \quad RMSE_{\theta}^{IP,Traj_i} = \sqrt{\frac{\oint(\theta_{real}-\theta)^2 d\sigma}{\oint d\sigma}}, \quad RMSE_{\psi}^{IP,Traj_i} = \sqrt{\frac{\oint(\psi_{real}-\psi)^2 d\sigma}{\oint d\sigma}} \tag{9}$$

It is worth mentioning that even in the most demanding scenarios, the disparity between the estimated attitude and the actual attitude is less precise for the roll angle while it is accurate for pitch and yaw angles, while it .

In Table 2, the Root Mean Squared Errors (RMSE) for the three Euler angles are presented, considering various trajectories and inclination path angles. The first column represents the inclination path angle, and the second column displays the corresponding errors. Subsequent columns provide the numerical values of these errors for different trajectory types. To offer a concise summary, the last three rows showcase RMSEs for the set of inclination path angles in the same column. Similarly, the last column (Total) presents the total RMSEs for the set of trajectories in the same row. This comprehensive analysis provides insights into the accuracy of the attitude estimation across different scenarios.

It is crucial to emphasize that the Root Mean Squared Errors (RMSE) obtained for all the considered measures are exceptionally small, providing strong support for the practicality of the proposed methodology in accurately estimating the attitude of UAVs in a cost-effective manner. Specifically, the range of $RMSE_{\psi}^{IP,Traj_i}$ is from 0° to $5 \cdot 10^{-5\circ}$, $RMSE_{\theta}^{IP,Traj_i}$ is confined within 0° and $9 \cdot 10^{-3\circ}$, and $RMSE_{\phi}^{IP,Traj_i}$ is limited to 0° to

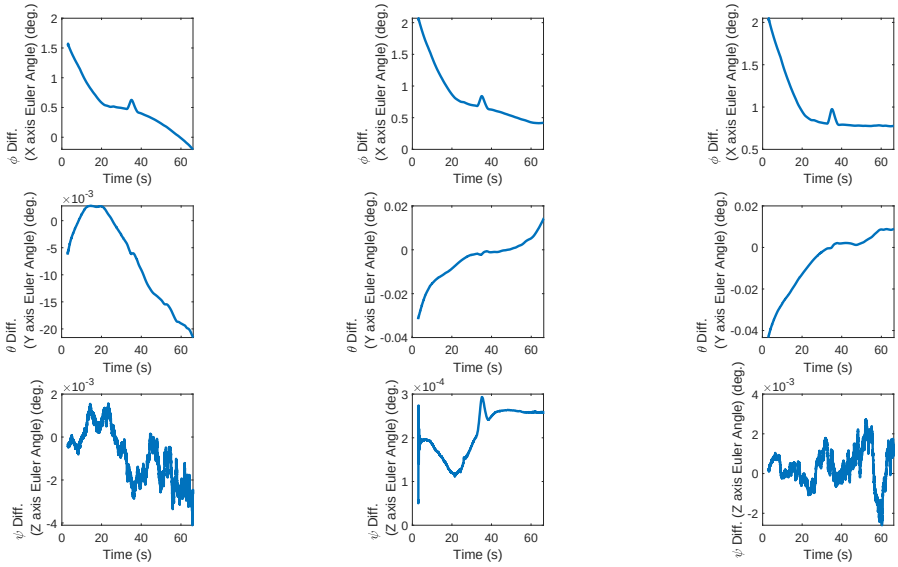

Figure 3: Contrasting the computed and true values for Euler Angles.

Table 2: Root Mean Squared Errors along the whole trajectory for a set of inclination path angles and for the 3 trajectories tested and calculation of a representative mean parameter.

		Trajectory			
Inclination Path (°)		1	2	3	Total
0	$RMSE_{\phi}^{IP,Traj_i}$	1.14E-02	1.13E-02	1.27E-02	6.80E-03
0	$RMSE_{\theta}^{IP,Traj_i}$	1.50E-03	1.99E-03	1.43E-03	9.60E-04
0	$RMSE_{\psi}^{IP,Traj_i}$	4.81E-05	8.98E-05	9.03E-05	4.54E-05
2,5	$RMSE_{\phi}^{IP,Traj_i}$	1.18E-02	1.30E-02	1.45E-02	7.59E-03
2,5	$RMSE_{\theta}^{IP,Traj_i}$	2.97E-03	2.61E-03	3.65E-03	1.79E-03
2,5	$RMSE_{\psi}^{IP,Traj_i}$	1.01E-04	3.66E-05	6.27E-05	4.14E-05
5	$RMSE_{\phi}^{IP,Traj_i}$	1.33E-02	1.20E-02	1.53E-02	7.86E-03
5	$RMSE_{\theta}^{IP,Traj_i}$	3.74E-03	3.05E-03	3.28E-03	1.95E-03
5	$RMSE_{\psi}^{IP,Traj_i}$	6.40E-05	1.05E-04	3.89E-05	4.29E-05
7,5	$RMSE_{\phi}^{IP,Traj_i}$	9.90E-03	9.09E-03	1.11E-02	5.81E-03
7,5	$RMSE_{\theta}^{IP,Traj_i}$	1.97E-03	4.74E-04	1.38E-03	8.16E-04
7,5	$RMSE_{\psi}^{IP,Traj_i}$	5.12E-05	2.25E-05	3.81E-05	2.26E-05
10	$RMSE_{\phi}^{IP,Traj_i}$	5.82E-03	5.17E-03	7.73E-03	3.66E-03
10	$RMSE_{\theta}^{IP,Traj_i}$	1.44E-03	1.94E-03	2.12E-03	1.07E-03
10	$RMSE_{\psi}^{IP,Traj_i}$	2.11E-06	6.06E-05	9.48E-05	3.75E-05
Total	$RMSE_{\phi}^{IP,Traj_i}$	4.81E-03	4.69E-03	5.61E-03	2.92E-03
Total	$RMSE_{\theta}^{IP,Traj_i}$	1.11E-03	9.81E-04	1.14E-03	6.24E-04
Total	$RMSE_{\psi}^{IP,Traj_i}$	2.77E-05	3.13E-05	3.10E-05	1.74E-05

$6 \cdot 10^{-3\circ}$. These outcomes affirm that, when applied to this specific set of sensors and attitude determination vectors, the algorithms exhibit heightened precision in measurements related to yaw and pitch angles and comparatively less precision for the roll angle. This level of accuracy underscores the potential of the proposed approach for reliable and cost-effective attitude estimation in unmanned air vehicle applications.

7 CONCLUSIONS AND FUTURE WORK

An innovative and cost-efficient method for evaluating the attitude of unmanned air vehicles has been introduced. This technique involves estimating two distinct vectors—velocity and vector of gravitys—measured and assessed in two reference trihedra using a GNSS sensor and a set of accelerometers. Additionally, a strategy for estimating the vector of gravity based on neural networks has been outlined. There are ongoing efforts to extend this methodology to various types of both conventional and unconventional aircraft, though this expansion is reserved for a more comprehensive study.

Nonlinear simulations have been conducted for UAV trajectories to obtain the 'real' attitude, which is then compared with the attitude derived from the proposed approach. Computational results indicate that differences are sufficiently minimal, positioning the presented algorithm as a promising candidate for integration into a control algorithm. Notably, the overall root mean square errors, as depicted in Table 2, consistently remain below 0.01° for all three attitude angles across various cases.

The proposed computation is particularly relevant for UAVs and/or spinning vehicles, especially in scenarios where other low-cost approaches, such as those involving magnetometers, are impractical due to electronic interference with other components in unmanned air vehicles. The cost-effectiveness of the components involved further enhances the attractiveness of this approach for numerous low-cost professional applications.

ACKNOWLEDGMENTS

This work was supported in part by the "Agencia Estatal de Investigación in Spain (MCIN/AEI/10.13039/501100011033)" Project under Grant PID2020-112967GB-C33, in part by the "NextGenerationEU" Project under Grant TED2021-130347B-I00, in part by Rey Juan Carlos University Project under Grant 2023/00004/010-F919, and in part by the "Unión Europea–Next Generation EU" Project under Grant URJC-AI-22.

REFERENCES

Azar, A. T., A. Koubaa, N. Ali Mohamed, H. A. Ibrahim, Z. F. Ibrahim, M. Kazim, , , , *et al*. 2021. "Drone deep reinforcement learning: A review". *Electronics* 10(9):999.

Crassidis, J. L., F. L. Markley, and Y. Cheng. 2007. "Survey of nonlinear attitude estimation methods". *Journal of guidance, control, and dynamics* 30(1):12–28.

de Celis, R. and L. Cadarso. 2018. "An estimator for UAV attitude determination based on accelerometers, GNSS sensors, and aerodynamic coefficients". *Navigation: Journal of The Institute of Navigation* 65(3):319–334.

de Celis, R. and L. Cadarso. 2023. "Neural Network-Based Controller For Terminal Guidance Applied In Short-Range Rockets". *IEEE Aerospace and Electronic Systems Magazine* 38(4):28–42.

de Celis, R., L. Cadarso, and J. Sánchez. 2017. "Guidance and control for high dynamic rotating artillery rockets". *Aerospace Science and Technology* 64:204–212.

Eure, K. W., C. C. Quach, S. L. Vazquez, E. F. Hogge and B. L. Hill. 2013. "An application of UAV attitude estimation using a low-cost inertial navigation system". Technical report.

Gebre-Egziabher, D., G. H. Elkaim, J. Powell, and B. W. Parkinson. 2000. "A gyro-free quaternion-based attitude determination system suitable for implementation using low cost sensors". In *IEEE 2000. Position Location and Navigation Symposium (Cat. No. 00CH37062)*, 185–192. IEEE.

Henkel, P. and M. Iafrancesco. 2014. "Tightly coupled position and attitude determination with two low-cost GNSS receivers". In *2014 11th International Symposium on Wireless Communications Systems (ISWCS)*, 895–900. IEEE.

MacKay, D. J. 1992. "Bayesian interpolation". *Neural computation* 4(3):415–447.

Mizell, D. 2003. "Using gravity to estimate accelerometer orientation". In *Seventh IEEE International Symposium on Wearable Computers, 2003. Proceedings.*, 252–252. Citeseer.

Møller, M. F. 1993. "A scaled conjugate gradient algorithm for fast supervised learning". *Neural networks* 6(4):525–533.

Moré, J. J. 2006. "The Levenberg-Marquardt algorithm: implementation and theory". In *Numerical analysis: proceedings of the biennial Conference held at Dundee, June 28–July 1, 1977*, 105–116. Springer.

Nawaz, A., H. Zhiqiu, W. Senzhang, Y. Hussain, I. Khan and Z. Khan. 2020. "Convolutional LSTM based transportation mode learning from raw GPS trajectories". *IET Intelligent Transport Systems* 14(6):570–577.

Pachter, M., T. C. Welker, and R. E. Huffman Jr. 2013. "Gyro-Free INS Theory". *NAVIGATION: Journal of the Institute of Navigation* 60(2):85–96.

Pang, Y., N. Xu, and Y. Liu. 2019. "Aircraft trajectory prediction using LSTM neural network with embedded convolutional layer". In *Proceedings of the Annual Conference of the PHM Society*, Volume 11, 1–8. PHM Society Scottsdale, AZ, USA.

Raskaliyev, A., S. H. Patel, T. M. Sobh, and A. Ibrayev. 2020. "GNSS-based attitude determination techniques—a comprehensive literature survey". *Ieee Access* 8:24873–24886.

Savage, P. G. *et al*. 2000. *Strapdown analytics*, Volume 2. Strapdown Associates Maple Plain, MN.

Silvestrini, S and Lavagna, M. "Deep Learning and Artificial Neural Networks for Spacecraft Dynamics, Navigation and Control. Drones 2022, 6, 270".

Springmann, J. C. and J. W. Cutler. 2014. "Flight results of a low-cost attitude determination system". *Acta Astronautica* 99:201–214.

Sun, X., X. Mao, and P. Chen. 2022. "High-precision attitude determination using spaceborne gravity gradiometer and gyroscope". *Acta Astronautica* 200:213–225.

Wahba, G. 1965. "A least squares estimate of satellite attitude". *SIAM review* 7(3):409–409.

Yin, X., X. Peng, G. Zhang, B. Che and M. Tang. 2022. "Research on Attitude Control System Design and Flight Experiments of Small-scale Unmanned Aerial Vehicle". In *2022 34th Chinese Control and Decision Conference (CCDC)*, 5866–5871. IEEE.

Yu, X., Y. Fu, P. Li, and Y. Zhang. 2017. "Fault-tolerant aircraft control based on self-constructing fuzzy neural networks and multivariable SMC under actuator faults". *IEEE Transactions on Fuzzy Systems* 26(4):2324–2335.

Zhu, F., Z. Hu, W. Liu, and X. Zhang. 2019. "Dual-antenna GNSS integrated with MEMS for reliable and continuous attitude determination in challenged environments". *IEEE Sensors Journal* 19(9):3449–3461.

Zountouridou, E., G. Kiokes, A. Dimeas, J. Prousalidis and N. Hatziargyriou. 2023. "A guide to unmanned aerial vehicles performance analysis—the MQ-9 unmanned air vehicle case study". *The Journal of Engineering* 2023(6):e12270.

AUTHOR BIOGRAPHIES

RAUL DE CELIS is an associate professor in aerospace area at Rey Juan Carlos University. He received his Ph.D. degree from Universidad Rey Juan Carlos in December 2017. His research interests are model development of aeronautic systems and navigation and control for aerial platforms. His email address is raul.decelis@urjc.es.

LUIS CADARSO is an associate professor in aerospace area at Rey Juan Carlos University. He received the Ph.D. degree in Aerospace Engineering from the Technical University of Madrid, Spain. His research interests include operations research, navigation, and control for aerial platforms. His email address is luis.cadarso@urjc.es.